

Inter-Regional Correlation in Tree-Growth Variations in the Western United States, 1513-1964, at ENSO, Sunspot, and Longer Frequency Bands

David M. Meko

Abstract: Cross-spectral analysis of regional tree-ring data suggests the spatial pattern of correlation between moisture variations in the Sierra Nevada of central California and in other parts of the western United States is frequency dependent. Short wavelengths (2.8 to 10.7 years), perhaps associated with El Niño/Southern Oscillation, are strongly coherent both to the north (Oregon) and to the south (Southern California). Longer wavelengths (45 to 75 years) are strongly coherent only to the north. Frequency bands corresponding to annual sunspot series were associated with relatively weak patterns of spatial correlation.

Introduction

Indices of ring-widths from drought-sensitive trees provide proxy climatic series several centuries long over much of the mountainous western United States (Stockton *et al.* 1985). These data are particularly useful for their unique information on climate variations on decadal-and-longer time scales. One type of question that can be addressed with tree-ring data is whether growth variations (and inferred moisture variations) in major runoff-producing areas have marched in step with major swings of known geophysical or astronomical time series. Such linkage would have important implications for water resources planning.

In this paper, tree-growth variations in the Sierra Nevada mountains of central California are compared with variations in other regions of the western United States using cross-spectral analysis. The significance of inter-regional correlation in growth is tested at four specific frequency bands associated with the following phenomena: El Niño/Southern Oscillation (ENSO), annual sunspot series, double sunspot series, and "long-wave" features.

Tree-Ring Data

Forty-one chronologies of ring-width indices, all covering the period 1700-1964, were grouped into five regions (Figure 1). The central California Sierras, region 2, is the focus of this paper. Other regions are referred to as Oregon (1), Southern California (3), Wyoming (4), and Colorado (5). A subset of 26 of these chronologies (Table 1) provided time coverage for AD 1513-1964, the period of analysis for this study. A preliminary correlation analysis showed the 1513-1964 subset was representative of growth variations of the full set for 1700-1964 in each of the five regions. The first eigenvector of growth, 1513-1964, in each region was used to weight the chronologies into regional growth series. To facilitate interregional comparison, regional growth series were then standardized to zero mean and unit variance.

Figure 1
LOCATIONS OF TREE-RING SITES
PROVIDING COVERAGE FOR
AD 1513-1964 (Δ) AND AD 1700-1964 (+)

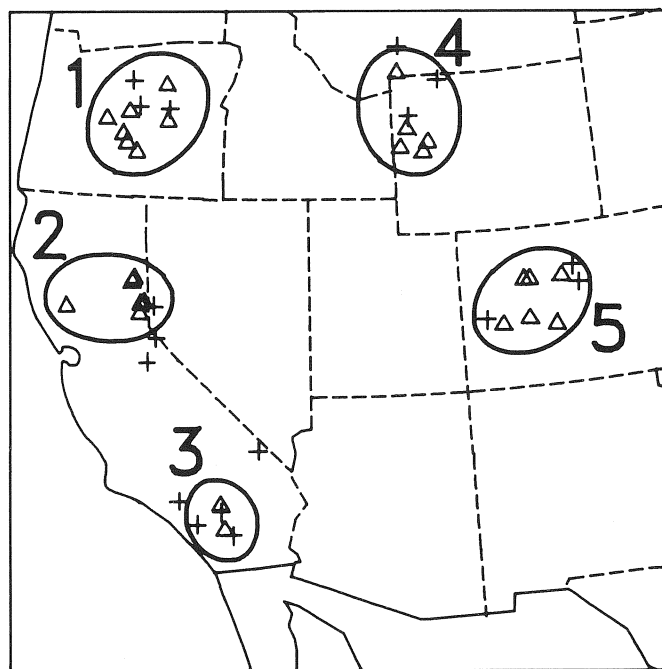


Table 1
IDENTIFICATION NUMBER, STATE,
REGION, AND SPECIES CODE FOR
EACH TREE-RING CHRONOLOGY
USED IN THE STUDY

Identifi- cation	State	Region	Species
SPR661	OR	1	Western Juniper
CAL661	OR	1	Western Juniper
COM661	OR	1	Western Juniper
FRE661	OR	1	Western Juniper
HOR661	OR	1	Western Juniper
LIT661	OR	1	Western Juniper
LOS641	OR	1	Ponderosa Pine
394649	CA	2	Jeffrey Pine
LEM571	CA	2	Jeffrey Pine
ANT571	CA	2	Jeffrey Pine
ANT641	CA	2	Ponderosa Pine
DON571	CA	2	Jeffrey Pine
SJM641	CA	2	Ponderosa Pine
005520	CA	3	Big-Cone Spruce
006649	CA	3	Ponderosa Pine
GRDDF9	MT	4	Mixed
282540	WY	4	Mixed
283590	WY	4	Limber Pine
051549	WY	4	Douglas Fir
552590	WY	4	Limber Pine
112549	CO	5	Douglas Fir
118629	CO	5	Undetermined Pine sp.
121549	CO	5	Douglas Fir
115549	CO	5	Douglas Fir
116549	CO	5	Douglas Fir
113629	CO	5	Pinyon Pine

Methods

Spectral and cross-spectral analysis of regional growth series followed methodology described in Bloomfield (1976). The purpose of the spectral analysis was to display the distribution of variance as a function of frequency, rather than to test for periodicity. Each regional series was prepared for spectral analysis by subtracting its mean, tapering 5% of the data on each end with a raised-cosine filter, and padding with zeros to length 512 years. The periodogram was computed using a fast Fourier transform algorithm, then smoothed successively by 5-weight and 7-weight Daniell filters to produce the estimated spectrum. Approximate 95% confidence limits for spectral estimates were calculated based on the assumption of a chi-squared distribution (page 196 in Bloomfield 1976). A null continuum was computed by smoothing the periodogram successively with two very broad (length 33 and 77) Daniell filters.

Cross-spectral estimates were also based on periodogram smoothing, although in this case by rectangular rather than Daniell filters, and series were not padded or tapered beforehand. Therefore, sample length was 452 years, with Fourier frequencies at $0/452$, $1/452$, $2/452$, ... and $0.5 \text{ cycle yr}^{-1}$.

Lengths of periodogram filters were chosen to bracket the desired range of wavelengths for each key frequency. The exact endpoints of these ranges are necessarily dependent on the discrete frequencies at which periodogram estimates are available for the given sample size (452 years). Filter lengths and characteristics are listed in Table 2.

Filter	Number of Weights	Central		Period Range (yrs)
		Period (yrs)	Frequency (yr ⁻¹)	
1	5	56.5	0.0177	45 - 75
2	9	22.6	0.0442	18.8 - 28.3
3	17	11.0	0.0907	9.2 - 13.7
4	119	4.4	0.2235	2.8 - 10.8

The percentage of tree-ring variance for region 2 in each of the four key frequency bands was computed by summing the appropriate range of raw-periodogram ordinates and dividing by the total variance.

The significance test on which this paper focuses is based on the estimated squared-coherence from cross-spectral analysis. Let $s_{X,Y}(\omega)^2$ be the sample squared-coherence and $r_{X,Y}(\omega)$ be the theoretical coherence. If $r_{X,Y}(\omega) \neq 0$, the probability of a sample squared-coherence being less than a given level $\sigma(p)^2$ is p , where:

$$\sigma(p)^2 = 1 - (1-p) g^2 / (1-g^2)$$

If the time series has not been tapered or padded, the quantity g^2 in the above equation is simply equal to the sum of the squares of the weights of the function used to smooth the periodogram. For example, for the 5-weight rectangular filter, each weight is 0.2, the sum of squares of weights equals 0.2, and the 95% and 99.9999% confidence limits for squared-coherence are:

$$\sigma(0.999999)^2 = 1 - (1 - 0.999999) 0.2 / (1 - 0.2) = 0.53$$

$$\sigma(0.999999)^2 = 1 - (1 - 0.999999) 0.2 / (1 - 0.2) = 0.97$$

Results

The tree-ring time series for region 2 shows considerable large-amplitude swings from the mean, especially in the last 100 years: prominent troughs in growth are located at about 1870 and 1940, and peaks in the early 1900s and near 1960 (Figure 2). The corresponding spectrum is predominantly low frequency, with a maximum near a wavelength of 64 years (Figure 3). Frequencies near the single and double sunspot cycles have spectral peaks, but the 95% confidence band around these still includes the null continuum.

Spectra of growth for the other four regions are similarly dominated by variance at low frequencies (Figure 4). In regions 1, 4, and 5 the highest peak is also the lowest-frequency peak. This peak is at the same wavelength (64 years) for the Oregon and central California series, but shortens to 51.2 years for Wyoming and lengthens to 102 years for Colorado.

Figure 2
INDEX OF REGIONAL TREE GROWTH VARIATIONS FOR REGION 2
STANDARDIZED TO ZERO MEAN AND UNIT STANDARD DEVIATION

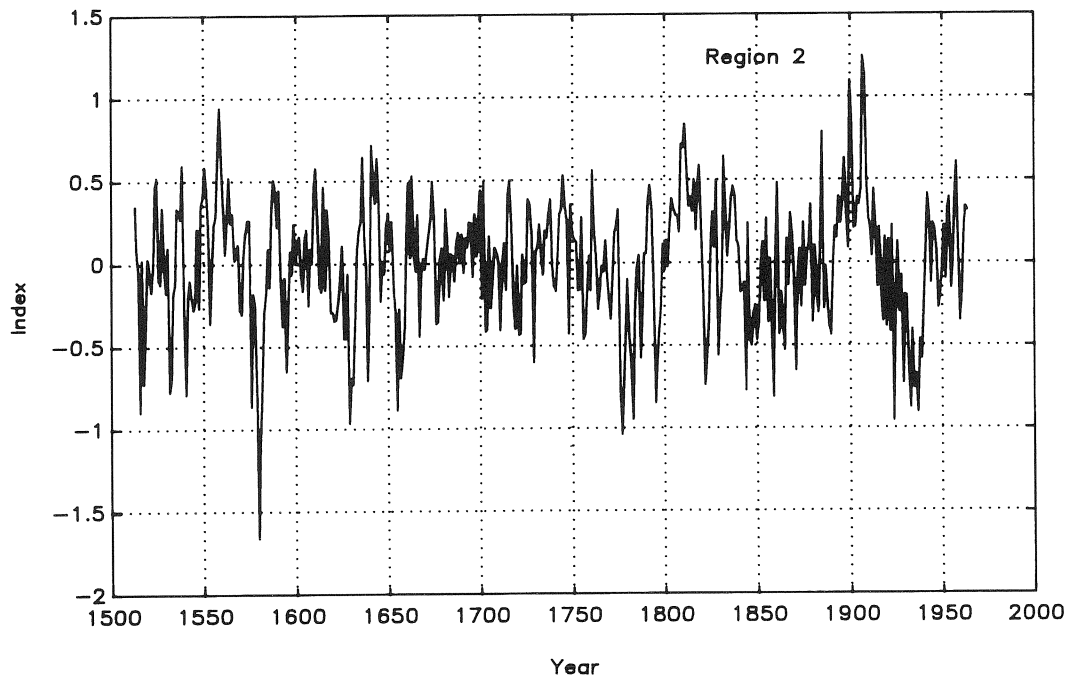


Figure 3
ESTIMATED SPECTRUM OF TREE-RING INDEX FOR REGION 2

Also shown are 95% confidence bands around the spectral estimates, a smooth underlying null continuum, and the raw periodogram ordinates (+). The window used to smooth the raw periodogram to estimate the spectrum is inset.

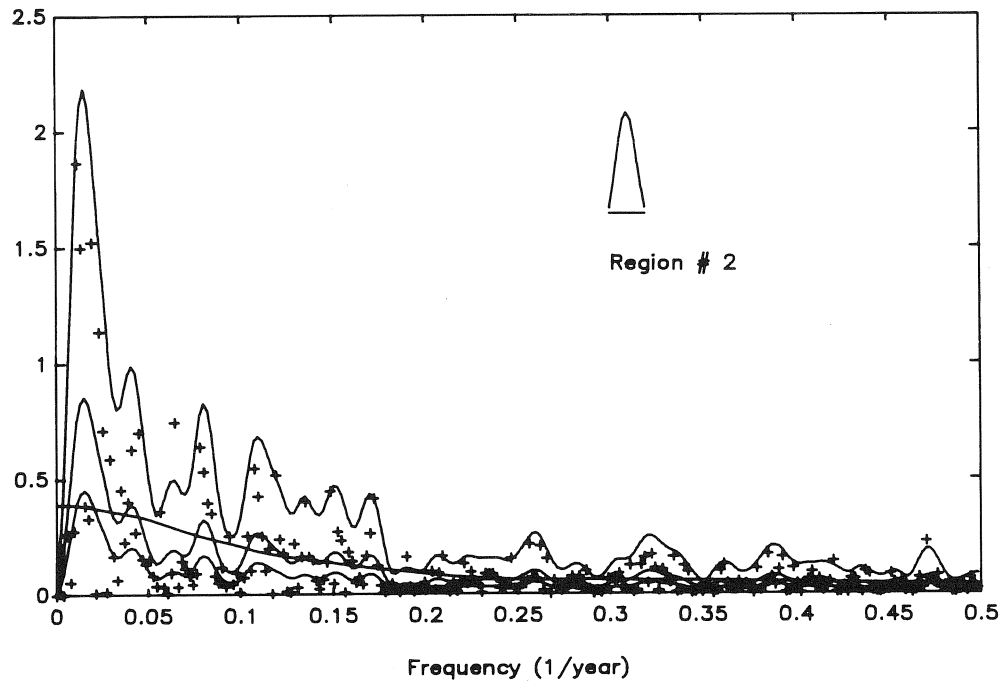
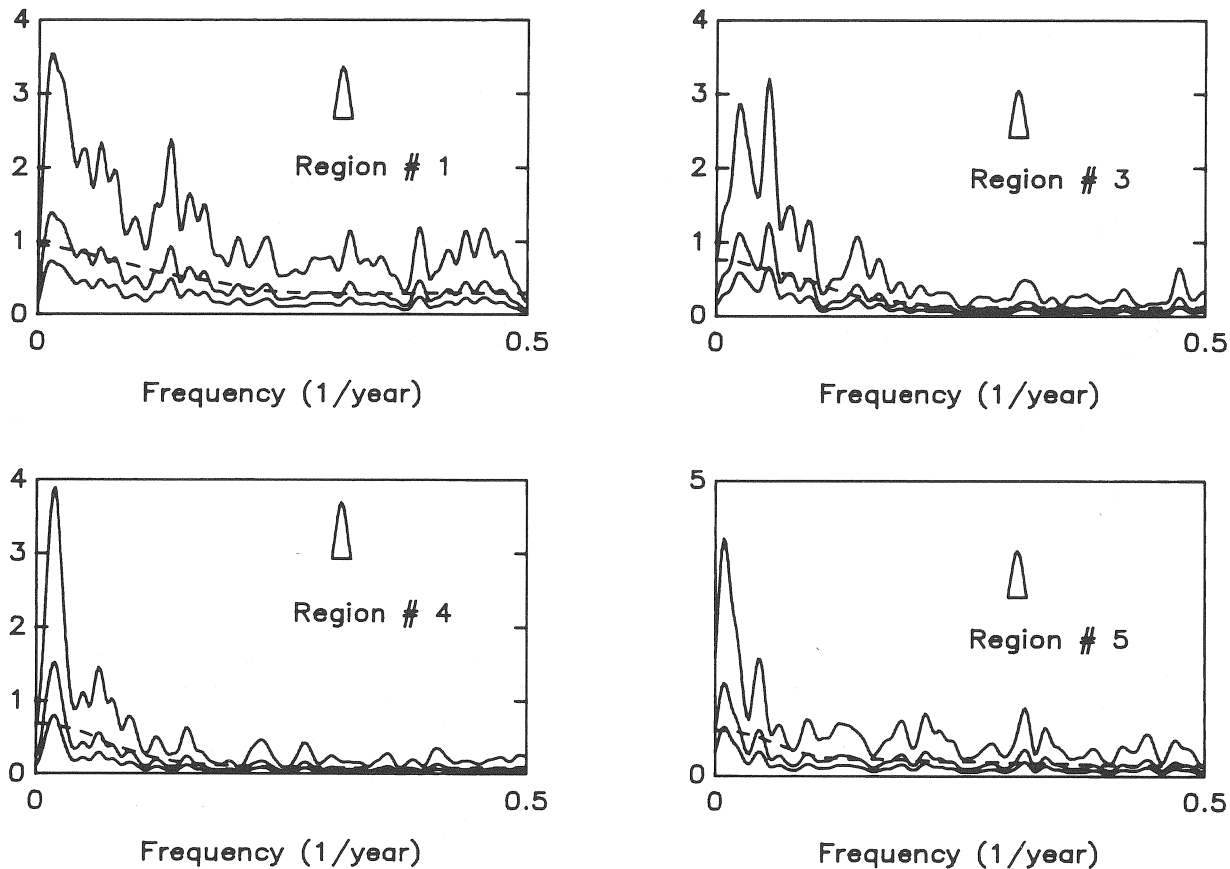


Figure 4
ESTIMATED SPECTRA, 95% CONFIDENCE BANDS, AND NULL CONTINUUM FOR
REGIONAL GROWTH SERIES, REGIONS 1,3,4,5

The periodogram smoothing window is inset on each figure. Series for region 5 is plotted with slightly compressed y-scale relative to other series.



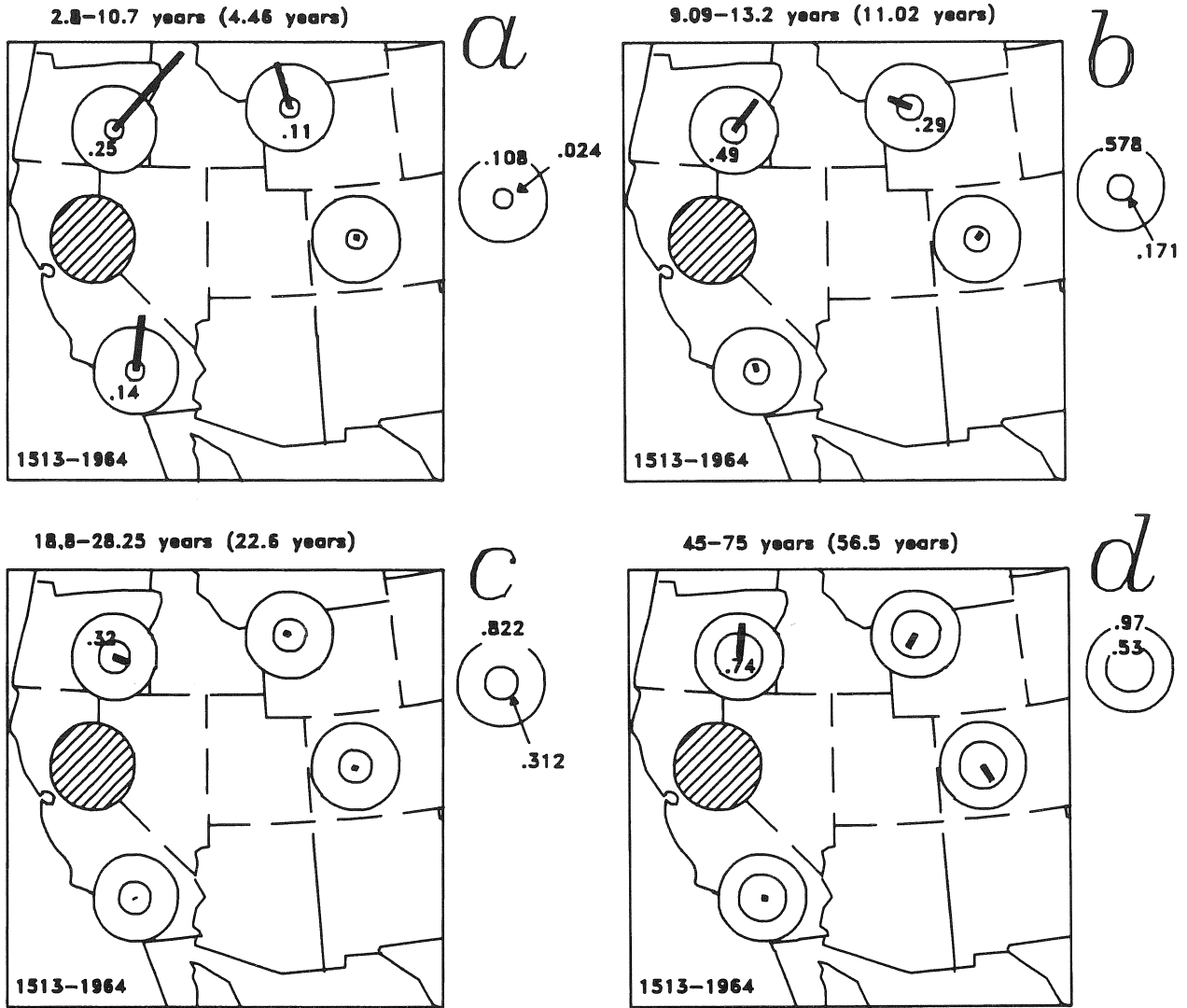
The southern California (region 3) spectrum differs markedly from the others in that the main variance component is shifted from very low to intermediate frequencies. Here the two dominant peaks are at 18.3 years and 39.4 years.

The method used to display the cross-spectral results was to plot estimated squared-coherence as bars on a series of maps (Figure 5). A separate map is shown for each key frequency-range. Length of a bar is proportional to the squared-coherence of a region's growth series with the series from central California. Angle of the bar from the vertical is proportional to the phase: straight up indicates growth variations are perfectly in phase; straight down indicates opposite (180 degrees out of) phase. Significance of the squared-coherence is found by comparing the length of the bar to radii of circles drawn at the 95% and 99.9999% confidence limits. For example, for the ENSO band (Figure 5a), the squared-coherence of region 1 with region 2 is highly significant and essentially in phase: the sample squared-coherence of 0.25 is expected less than 1 in a million times by chance (0.0001% confidence limit of 0.108).

The ENSO band represents 39% of the variance of the central California series. Growth variations in this band are strongly coherent and in phase with the Oregon, Wyoming, and southern California series (Figure 5a). Correlation drops below 95% significance with Colorado and Arizona.

Figure 5
MAPS SUMMARIZING RESULTS OF CROSS-SPECTRAL ANALYSIS OF
EACH REGIONAL GROWTH SERIES WITH THE SERIES FOR REGION 2

Shown are the estimated squared-coherence (bars), its 95% and 99.9999% confidence limits (circles), and the phase (angle from the vertical). A key to the magnitude of the specified confidence limits is shown in the circles to the right of each map. Squared-coherence values are listed on the maps when they exceed the 95% confidence limit.



The single-sunspot band represents 13% of the variance for central California. Significance of squared-coherence estimates is lower than for the ENSO band, though still exceeding 95% for Oregon and Wyoming (Figure 5b). The most striking difference from the plot for the ENSO band is that correlation drops below significance with southern California.

The double-sunspot band represents 9% of the variance for central California. This is the least spatially coherent of the four patterns (Figure 5c). The squared-coherence is barely significant at the 95% level with the Oregon series, and not significant with any other region. Even for the Oregon relationship, the series appear to be about one-quarter cycle, or 5 years, out of phase.

The 45-75 year band represents 12% of the variance for central California, about the same amount as the single-sunspot band. A strong in-phase relationship is shown with Oregon at this band (Figure 5d). In contrast to the ENSO frequency band, the correlation with southern California is essentially zero. The pattern of bars suggests the possibility of an opposite-phase relationship with the Wyoming and Colorado series at this band. One possible explanation, though highly speculative given the low significance levels of squared-coherence, is that long waves at this time-scale are preferably anchored such that the northeastern and northwestern regions were affected by opposing moisture regimes. Previous studies have shown a similarly large, spatially coherent, spectral feature at near 60 years in tree-ring data from the western fringe of the northern U.S. Great Plains (Meko 1982, Stockton and Meko 1983).

Conclusions

The results suggest a frequency dependence not only in the strength but also in the sign of correlation between moisture variations in the Sierra Nevada mountains of central California and in other regions. While variations in the ENSO frequency band (2.8-10.7 years) are strongly coherent and in-phase both to the north and south, variations at low frequencies (45-75 years) show in-phase coherence only to the north. Moreover, there is a hint of an opposite-phase relationship with moisture variations at low frequencies in the Colorado Rockies. No evidence was found of unusually distinct patterns of spatial correlation at either the single- or double-sunspot cycles. To some extent, this is negative evidence for a solar-climate signal, at least for the central California Sierras. A different picture could, of course, come from similar analyses keyed on other regions — for example, regions to the east not under such a strong winter-dominant precipitation regime as region 2.

Acknowledgment

This work was supported by the National Science Foundation, grant ATM-88-14675.

References

- Bloomfield, P. 1976. *Fourier Analysis of Time Series: An Introduction*. John Wiley & Sons.
- Meko, D.M. 1982. "Drought History in the Western Great Plains from Tree Rings". *Proceedings of the International Symposium on Hydrometeorology*. American Water Resources Association.
- Stockton, C.W., W.R. Boggess, and D.W. Meko. 1985. "Climate and Tree Rings". in *Paleoclimate Analysis and Modeling*. Ed. A.D. Hecht. John Wiley & Sons.
- Stockton, C.W., and D.M. Meko. 1983. "Drought Recurrence in the Great Plains as Reconstructed from Long-Term Tree-Ring Records". *J. of Climate and Applied Climatology* 22(1):17-29.